Excitation energies and transition rates in magnesiumlike ions

U. I. Safronova, W. R. Johnson, and H. G. Berry
Department of Physics, University of Notre Dame, Notre Dame, Indiana 46556
(Received 28 October 1999; published 7 April 2000)

Excitation energies, transition probabilities, and lifetimes are calculated for $3l_13l_2$-$3l_33l_4$ electric dipole transitions in Mg-like ions with nuclear charges Z ranging from 13 to 100. Relativistic many-body perturbation theory (MBPT), including the Breit interaction, is used to evaluate retarded $E1$ matrix elements in length and velocity forms. The calculations start from a $1s^22s^22p^6$ Dirac-Fock potential. First-order perturbation theory is used to obtain intermediate coupling coefficients, and the second-order MBPT is used to determine the matrix elements. The contributions from negative-energy states are included in the second-order $E1$ matrix elements to achieve agreement between length-form and velocity-form amplitudes. The resulting transition energies and lifetimes are compared with experimental values and with results from other recent calculations.

PACS number(s): 31.15.Md, 31.25.Jf, 31.30.Jv, 32.70.Cs

I. INTRODUCTION

The magnesium isoelectronic sequence has two valence electrons outside a closed $n=2$ core, and is a paradigm for studying strong correlations between closely spaced levels. There are many examples in this sequence of level crossings of states having the same parity and angular momentum; such examples occur for both low and high values of the nuclear charge Z. Notably, the $3p^2$, the $3p3d$, and the $3d^2$ levels cross the $3snl$ ($l=0$ to 4) levels, becoming relatively more tightly bound as the nuclear charge Z increases. Such crossings provide severe tests of atomic structure calculations. Comparisons with measurements of energies, transition rates, and fine-structure intervals also provide useful tests of the quality of different theoretical models. Many experimental energy levels and fine-structure intervals are now available up to very high nuclear charge ($Z=50$) for the $3l3l'$ levels; additionally, experimental rates for some transitions between these levels are available. The objective of this paper is to present a comprehensive set of calculations for $3l3l'$ energies and transition rates, and to compare them with previous calculations and experiments for the entire Mg isoelectronic sequence. Most earlier measurements and calculations focused on the $3snl\,^{1,3}L$ states and the low-lying $3p^2$ configuration of $^1S, ^1D$, and ^3P states. Very few results exist for other $3pnl$ states. The large number of possible transitions have made experimental identification difficult. With this more accurate set of calculations, experimental verifications should become simpler and more reliable.

Several early theoretical calculations for Mg-like ions were based on the Hartree-Fock method: excitation energies and line strengths for the low-lying states of ions in the sequence were studied using multiconfiguration Dirac-Fock (MCDF) wave functions by Cheng and Johnson [1] and lifetimes were evaluated using multiconfiguration Hartree-Fock wave function by Froese Fischer and Godefroid [2]. Recently, MCDF calculations of energies and transition probabilities along the Mg sequence were reported by Jönsson and Froese Fisher [3]. The multiconfiguration relativistic random-phase approximation (MCRRPA) was used by Huang and Johnson [4] to calculate excitation energies and oscillator strengths for Mg-like ions and by Chou, Chi, and Huang [5] to determine excitation energies and oscillator strengths including core-polarization effects in Mg-like ions with $Z=12$–22. Butler *et al.* [6] used a modified R-matrix program to calculate energies and oscillator strengths for some $3l3l'$ transitions in a limited number of ions ($Z=12$–14, 16, 18, 20, and 26); while Curtis [7] used a semiempirical method to obtain transition rates for the $3s^2$-$3s3p$ resonance and intercombination transitions for the entire sequence [7]. Finally, it should be noted that large-scale relativistic configuration-interaction (CI) calculations of $3s^2\,^1S_0$-$3s3p\,^{1,3}P_1$ transition energies in Mg-like ions were carried out recently by Chen and Cheng [8].

Accurate measurements along the Mg isoelectronic sequence come from a variety of light sources. Most accurate wavelength measurements come from plasma light sources, both magnetic-fusion and laser-produced plasmas, early work on the low-Z ions being completed by Fawcett [9]. Other early wavelength measurements on high-Z ions are by Litzen and Redfors [10], Churilov *et al.* [11], and by Sugar and Kaufman [12,13]. Much of this work was summarized by Ekberg *et al.* [14] in their report of measurements on Ge XXI–Zr XXIX observed in laser-produced plasmas [14], and which is compared with the present data in [15]. Seely *et al.* [16] studied the $3s^2\,^1S_0-3s3p\,^3P_1$ intercombination transition from Fe XV to Nd IL. Jupén *et al.* [17] reported results in Mg-like Kr and Mo obtained in the JET Tokamak.

Lifetime measurements along the Mg isoelectronic sequence are quite sparse and have focused on the $3s^2$-$3s3p$ resonance and intercombination transitions: Engström *et al.* [18], in recent beam-foil work in Cl VI, refer to previous work on these transitions in S V and Ar VII by Reistad *et al.* [19,20] and also in Fe XV and Ni XVII by Hutton *et al.* [21,22]. Baudinet-Robinet *et al.* [23] made lifetime measurements of most of the low-lying allowed transitions in Cl VI, while Träbert *et al.* [24] measured the resonance transition lifetime in Br XXIV. Quite recently, Träbert *et al.* [25] made an extensive set of lifetime measurements, including those for the $3p3d\,^3F$ states, in Mg-like calcium Ca IX. These experimental results are compared with our calculations below.

In the present paper, relativistic many-body perturbation

 ©2000 The American Physical Society

theory (MBPT) is used to determine energies of $n=3$ states of Mg-like ions with nuclear charges $Z=13$–100. Energies are calculated for the $3s^2$ ground state, the 18 even-parity $3p3p'$,$3s3d$, and $3d3d'$ excited states, and the 16 odd-parity $3s3p$ and $3p3d$ excited states. The calculations are carried out to second order in perturbation theory. Corrections for the (frequency-dependent) Breit interaction are included in first order only. Lamb shift corrections to energies are also estimated and included.

Relativistic MBPT is used to determine reduced matrix elements, oscillator strengths, and transition rates for all 168 allowed and forbidden electric dipole $3l$-$3l'$ transitions in Mg-like ions. Retarded $E1$ matrix elements are evaluated in both length and velocity forms. The MBPT calculations starting from a local potential are gauge independent order by order, providing ''derivative terms'' are included in the second- and higher-order matrix elements and careful attention is paid to negative-energy states. The present MBPT calculations start from a nonlocal $1s^22s^22p^6$ Dirac-Fock potential and consequently give gauge-dependent transition matrix elements. Second-order correlation corrections compensate almost exactly for the gauge dependence of the first-order matrix elements, leading to corrected matrix elements that differ by less than 1% in length and velocity forms throughout the periodic system.

II. THEORETICAL TECHNIQUE

The MBPT formalism developed previously [26,27] for Be-like ions is used here to describe the perturbed wave functions, to obtain the second-order energies [26], and to evaluate the first- and second-order transition matrix elements in Mg-like ions. Differences between calculations for Be-like and Mg-like ions are due to the increased size of the model space ($3l3l'$ instead of $2l2l'$) and the Dirac-Fock potential ($1s^22s^22p^6$ instead of $1s^2$). These differences lead to much more laborious numerical calculations (35 states instead of 10 and 168 electric dipole transitions instead of 16).

A. Model space

The model space for the $n=3$ complex in Mg-like ions has 19 even-parity states and 16 odd-parity states. These states are summarized in Table I where both jj and LS designations are given. When starting calculations from relativistic Dirac-Fock wave functions, it is natural to use jj designations for uncoupled transition and energy matrix elements; however, neither jj nor LS coupling describes the *physical* states properly, except for the single-configuration state $3p_{3/2}3d_{5/2}(4)\equiv 3p3d\,^3F_4$.

Strong mixing between $3s3d_{3/2}(2)$ and $3p_{3/2}3p_{3/2}(2)$ states was discussed in detail by Cheng and Johnson [1]. Additionally, we found strong mixing inside the odd-parity complex of states. In Fig. 1, as an example, the mixing between the $3p_{1/2}3d_{5/2}(2)$ and $3p_{3/2}3d_{3/2}(2)$ states is illustrated. As can be seen from the figure, the dominant configuration for $Z=13$–31 is $3p_{3/2}3d_{3/2}(2)$ but changes to $3p_{1/2}3d_{5/2}(2)$ for $Z=32$–100.

TABLE I. Possible two-particle states in the $n=3$ complex.

Even-parity states		Odd-parity states	
jj coupling	LS coupling	jj coupling	LS coupling
$3s_{1/2}3s_{1/2}(0)$	$3s^2\,^1S_0$	$3s_{1/2}3p_{1/2}(0)$	$3s3p\,^3P_0$
$3p_{1/2}3p_{1/2}(0)$	$3p^2\,^3P_0$	$3p_{3/2}3d_{3/2}(0)$	$3p3d\,^3P_0$
$3p_{3/2}3p_{3/2}(0)$	$3p^2\,^1S_0$		
$3d_{3/2}3d_{3/2}(0)$	$3d^2\,^3P_0$		
$3d_{5/2}3d_{5/2}(0)$	$3d^2\,^1S_0$		
$3s_{1/2}3d_{3/2}(1)$	$3p^2\,^3P_1$	$3s_{1/2}3p_{1/2}(1)$	$3s3p\,^3P_1$
$3p_{1/2}3p_{3/2}(1)$	$3s3d\,^3P_1$	$3s_{1/2}3p_{3/2}(1)$	$3s3p\,^1P_1$
$3d_{3/2}3d_{5/2}(1)$	$3d^2\,^3P_1$	$3p_{1/2}3d_{3/2}(1)$	$3p3d\,^3P_1$
		$3p_{3/2}3d_{3/2}(1)$	$3p3d\,^3D_1$
		$3p_{3/2}3d_{5/2}(1)$	$3p3d\,^1P_1$
$3s_{1/2}3d_{3/2}(2)$	$3p^2\,^1D_2$	$3s_{1/2}3p_{3/2}(2)$	$3s3p\,^3P_2$
$3s_{1/2}3d_{5/2}(2)$	$3p^2\,^3P_2$	$3p_{1/2}3d_{3/2}(2)$	$3p3d\,^3F_2$
$3p_{1/2}3p_{3/2}(2)$	$3s3d\,^3D_2$	$3p_{1/2}3d_{5/2}(2)$	$3p3d\,^1D_2$
$3p_{3/2}3p_{3/2}(2)$	$3s3d\,^1D_2$	$3p_{3/2}3d_{3/2}(2)$	$3p3d\,^3P_2$
$3d_{3/2}3d_{3/2}(2)$	$3d^2\,^3F_2$	$3p_{3/2}3d_{5/2}(2)$	$3p3d\,^3D_2$
$3d_{5/2}3d_{5/2}(2)$	$3d^2\,^3P_2$		
$3d_{3/2}3d_{5/2}(2)$	$3d^2\,^1D_2$		
$3s_{1/2}3d_{5/2}(3)$	$3s3d\,^3D_3$	$3p_{1/2}3d_{5/2}(3)$	$3p3d\,^3F_3$
$3d_{3/2}3d_{5/2}(3)$	$3d^2\,^3F_3$	$3p_{3/2}3d_{3/2}(3)$	$3p3d\,^3D_3$
		$3p_{3/2}3d_{5/2}(3)$	$3p3d\,^1F_3$
$3d_{5/2}3d_{5/2}(4)$	$3d^2\,^3F_4$	$3p_{3/2}3d_{5/2}(4)$	$3p3d\ \ ^3F_4$
$3d_{3/2}3d_{5/2}(4)$	$3d^2\,^1G_4$		

B. Electric dipole transitions

We designate the first-order dipole matrix element by $Z^{(1)}$, the Coulomb correction to the second-order matrix element $Z^{(2)}$, and the second-order Breit correction $B^{(2)}$. The evaluation of $Z^{(1)}$,$Z^{(2)}$, and $B^{(2)}$ for Mg-like ions follows the pattern of the corresponding calculation for berylliumlike ions in Refs. [27,28]. These matrix elements are calculated in both length and velocity gauges. The differences between length and velocity forms are illustrated for the uncoupled $3s3s(0)$-$3s3p_{1/2}(1)$ matrix element in Fig. 2. It should be noted that the first-order matrix element $Z^{(1)}$ is proportional $1/Z$, the second-order Coulomb matrix element $Z^{(2)}$ is proportional $1/Z^2$, and the second-order Breit matrix element

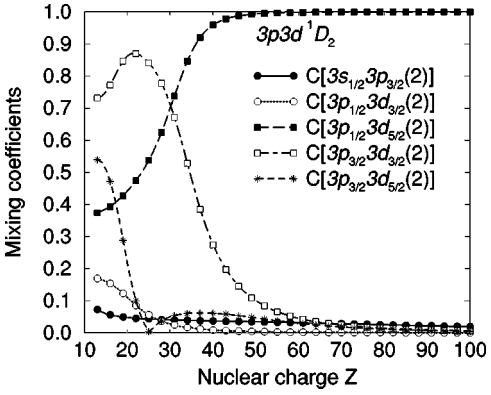

FIG. 1. Mixing coefficients for the $3p3d\,^1D_2$ level as functions of Z.

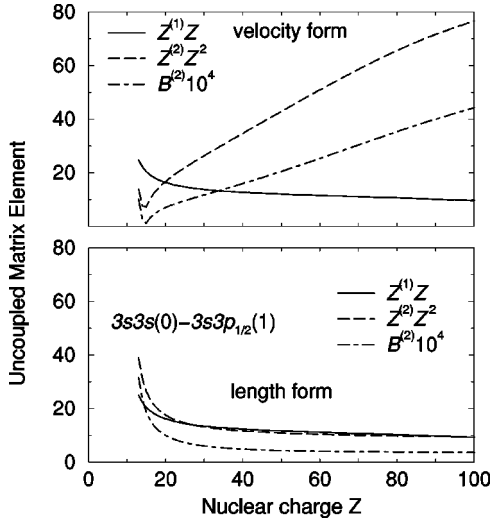

FIG. 2. Uncoupled matrix element for $3s3s(0)-3s3p_{1/2}(1)$ calculated in length and velocity forms.

$B^{(2)}$ is almost independent of Z (see [27]). Taking into account this dependence, $Z^{(1)}\times Z, Z^{(2)}\times Z^2$, and $B^{(2)}\times 10^4$ are shown in the figure. These Z dependences apply to the second-order matrix elements $Z^{(2)}$ and $B^{(2)}$ calculated in length form only. The contribution of the second-order matrix elements $Z^{(2)}$ and $B^{(2)}$ is much larger in velocity form (compare the upper and lower panels in Fig. 2). The differences between length- and velocity-form results in Fig. 2 are compensated by ''derivative terms'' $P^{(\mathrm{derv})}$, as shown later. It should be noted that $P^{(\mathrm{derv})}$ in length form almost equals $Z^{(1)}$ in length form; $P^{(\mathrm{derv})}$ in velocity form is smaller than $Z^{(1)}$ in velocity form by three to four orders of magnitude.

C. Contribution from the negative-energy states

As emphasized recently in studies of $E1$ transitions in Be-like ions [27,28], relativistic calculations require a careful treatment of negative-energy states (NESs). In this paper, we use the *no-pair* Hamiltonian [29–31], which excludes negative-energy states, to calculate relativistic wave functions. Negative-energy states contribute to transition amplitudes in higher-order MBPT calculations through sums over intermediate states [32]. To illustrate the relative importance of the NES contributions for Mg-like ions, consider length-form (S_L) and velocity-form (S_V) line strengths for the $3s^2\,{}^1S_0-3s3p\,{}^3P_1$ transition. Without NES contributions, the differences between S_L and S_V range from 25% at low Z to 5% at high Z; including NES contributions reduces the difference to less than 1% for all Z. Contributions from the negative-energy states are more important for S_V than for S_L. Essentially all of the length-velocity difference mentioned above is accounted for by NES contributions to S_V only.

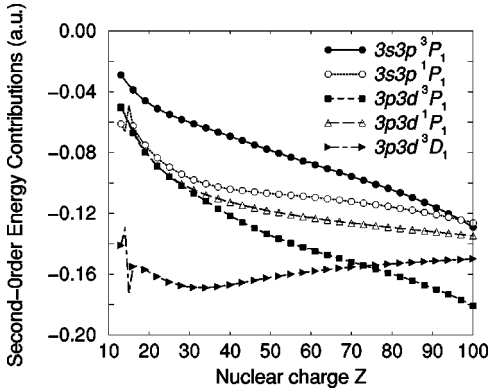

FIG. 3. Z dependence of the second-order energy contribution for the complex of odd-parity states with $J=1$.

D. Excitation energy

Details of the theoretical method used to evaluate second-order energies have been presented previously in [26] for Be-like ions. The energy calculations for Mg-like ions are illustrated in Table II and in Fig. 3. In Table II we list the following contributions to the energies of odd-parity $J=1$ states in Fe^{+14}: $E^{(0+1)}=E^{(0)}+E^{(1)},B^{(1)}$, the second-order Coulomb energy $E^{(2)}$, the QED correction $E^{(\mathrm{Lamb})}$, and the total theoretical energy $E^{(\mathrm{tot})}$. The screened self-energy and vacuum polarization data given by Blundell [33] are used to determine the QED correction $E^{(\mathrm{Lamb})}$. It should be noted that $E^{(\mathrm{tot})}$ for the ground state of Fe^{+22} is equal to $-34.733\,241$ a.u. and should be subtracted from the final column in Table II to obtain excitation energies relative to the ground state. This table illustrates that $E^{(2)}$ is the largest correction to the principal contribution $E^{(0+1)}$. In Fig. 3, we present the Z dependence of the $E^{(2)}$ corrections given in Table II. There are sharp features in the curves shown in Fig. 3 for $Z=14$ and 15 which can be explained by nonsymmetric off-diagonal terms in the second-order energy matrix discussed previously in Ref. [34].

III. COMPARISON OF RESULTS WITH OTHER THEORY AND EXPERIMENT

We calculate energies of the 16 odd-parity $3s_{1/2}3p_j(J)$ and $3p_j3d_{j'}(J)$ excited states, and the 19 even-parity

TABLE II. Energy of Fe^{+14} in a.u.

Level	$E^{(0+1)}$	$B^{(1)}$	$E^{(2)}$	$E^{(\mathrm{Lamb})}$	$E^{(\mathrm{tot})}$
$3s3p\,{}^3P_1$	−33.600970	0.013143	−0.056198	0.002859	−33.641166
$3s3p\,{}^1P_1$	−33.053698	0.011912	−0.091401	0.002886	−33.130301
$3p3d\,{}^3P_1$	−30.170476	0.011126	−0.097890	−0.000032	−30.257272
$3p3d\,{}^3D_1$	−30.108322	0.009270	−0.097422	0.000114	−30.196360
$3p3d\,{}^1P_1$	−29.687265	0.009558	−0.166183	0.000179	−29.843711

TABLE III. Comparison with experimental data of present and other theoretical energies for $3s3p\ ^{1,3}P_1$ states relative to the ground state in cm^{-1} for Mg-like ions.

	$3s3p\ ^3P_1$			$3s3p\ ^1P_1$		
Z	Present	Other	Expt.	Present	Other	Expt.
13	37818	37213 [a]	37454 [c]	59140	60104 [a]	59850 [c]
14	52840	52596 [a]	52758 [c]	81099	83104 [a]	82883 [c]
15	68231	67897 [a]	68139 [c]	107945	105398 [a]	105189 [c]
16	83186		83433 [c]	127492	127350 [a]	127149 [c]
17	98572		98700 [c]	149101	149175 [a]	148949 [c]
18	113893		113900 [c]	170778	170977 [a]	170720 [c]
18		113818 [b]			170692 [b]	
23	191444		191509 [d]	281448		281627 [d]
24	207367		207399 [e]	304476		304629 [e]
25	223442		223438 [f]	327907		328042 [f]
26	239682		239660 [g]	351804		351911 [g]
27	256099		256060 [h]	376231		376323 [h]
29	289492	289313 [b]	289401 [b]	426945	426962 [b]	426987 [b]
32	341051		340862 [i]	508800		508690 [i]
34	376423		376178 [i]	568220		568090 [i]
36	412583	412247 [b]	412290 [b]	632418	632250 [b]	632187 [b]
38	449508		449183 [i]	702253		701948 [i]
39	468248		467901 [i]	739573		739206 [i]
40	487167		486792 [i]	778654		778227 [i]
42	525529	525007 [b]	525028 [b]	862617	862188 [b]	862076 [b]

[a]Reference [3].
[b]Reference [8].
[c]Reference [36].
[d]Reference [37].
[e]Reference [38].
[f]Reference [39].
[g]Reference [40].
[h]Reference [41].
[i]Reference [14].

$3s^2_{1/2}(0), 3p_j 3p_{j'}(J)$, and $3s_{1/2}3d_j(J)$ excited states for Mg-like ions with nuclear charges ranging from $Z=13-100$. Reduced matrix elements, oscillator strengths, and transition rates are also determined for all 168 allowed and forbidden electric dipole $3l$-$3l'$ transitions for each ion. Comparisons are also given with other theoretical results and with experimental data. Our results are presented in three parts: transition energies, fine-structure energy differences, and transition probabilities and lifetimes.

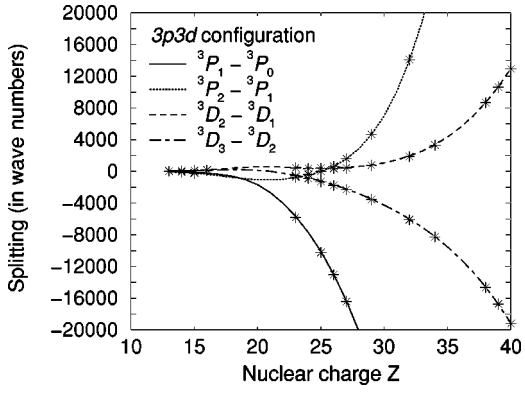

FIG. 4. The splitting (in cm^{-1}) of $3p3d\ ^3P$ and $3p3d\ ^3D$ terms as functions of Z;* are the NIST data Refs. [36]– [41].

TABLE IV. Comparison with experimental data of present and other theoretical fine-structure interval for the $3s3p\ ^3P_1$ term in cm^{-1} for Mg-like ions.

	$^3P_1$-$^3P_0$			$^3P_2$-$^3P_1$		
Z	Present	Other	Expt.	Present	Other	Expt.
13	61.5	60.5 [a]	60.9 [b]	124.6	123.2 [a]	123.9 [b]
14	128.6	127.6 [a]	128 [b]	262.2	260.8 [a]	261 [b]
15	228.9	227.4 [a]	227.4 [b]	470.4	467.5 [a]	468.4 [b]
16	369		362 [b]	764		767 [b]
17	558		552 [b]	1164		1165 [b]
18	804		805 [b]	1692		1681 [b]
19	1116			2377		
20	1502			3240		
21	1971			4315		
22	2531			5635		
23	3193		3198 [c]	7237		7228 [c]
24	3960		3955 [d]	9164		9158 [d]
25	4842		4834 [e]	11458		11467 [e]
26	5843		5818 [f]	14171		14160 [f]
27	6969		6979 [g]	17355		17354 [g]
28	8221			21069		
29	9601			25374		
30	11110			30341		
31	12746			36042		
32	14505		14478 [h]	42556		42559 [h]
33	16383			49966		
34	18375		18384 [h]	58359		58351 [h]
35	20474			67830		
36	22672			78478		
37	24961			90406		
38	27332		27298 [h]	103720		103754 [h]
39	29777		29741 [h]	118533		118501 [h]
40	32287		32230 [h]	134962		134945 [h]
41	34853			153129		
42	37468			173157		

[a]Reference [3].
[b]Reference [36].
[c]Reference [37].
[d]Reference [38].
[e]Reference [39].
[f]Reference [40].
[g]Reference [41].
[h]Reference [14].

A. Transition energies

The resonance transitions $3s^2\ ^1S_0 - 3s3p\ ^{1,3}P_J$ have been thoroughly investigated, theoretically and experimentally, for the Mg sequence. In Table III, our MBPT results of the $3s^2\ ^1S_0 - 3s3p\ ^{1,3}P_1$ transitions are compared with other calculations and with experiments. The recently published CI calculation of Chen and Cheng [8] gives results for four ions Ar^{+6},Cu^{+17},Kr^{+24}, and Mo^{+30}. Our results for Ar^{+6},Cu^{+17}, and Kr^{+24} ions agree with experiment at the same level of accuracy as the CI calculations. The differences between our MBPT results and the CI results for Mo^{+30} are explained by differences in the QED contributions (-4311 cm^{-1} instead of -4530 cm^{-1} for the $3s^2\ ^1S_0 - 3s3p\ ^3P_1$ transition and -4070 cm^{-1} instead of -4258 cm^{-1} for the $3s^2\ ^1S_0 3s^2\ ^1S_0 - 3s3p\ ^1P_1$ transition). Our estimate of the

TABLE V. Wavelengths λ (Å) and electric dipole transition rates, $A(s^{-1})$ for lines in Mg-like Fe: (a) present calculation (b) NIST data Ref. [40]. Numbers in brackets represent powers of 10.

Lower level	Upper level	Wavelength, λ		Transition rate A	
		a	b	a	b
$3s3p\ ^3P_1$	$3s3d\ ^1D_2$	191.75	191.41	3.17[08]	3.08[8]
$3s3p\ ^3P_2$	$3s3d\ ^1D_2$	197.11	196.74	1.54[07]	1.1 [7]
$3p^2\ ^1D_2$	$3p3d\ ^1F_3$	199.48	198.87	1.91[10]	2.79[10]
$3s3p\ ^3P_0$	$3s3d\ ^3D_1$	225.01	224.75	1.32[10]	1.38[10]
$3s3p\ ^3P_1$	$3s3d\ ^3D_2$	227.47	227.21	1.72[10]	1.80[10]
$3s3p\ ^3P_1$	$3s3d\ ^3D_1$	228.01	227.73	9.42[09]	9.90[9]
$3s3p\ ^3P_2$	$3s3d\ ^3D_3$	234.18	233.86	2.11[10]	2.39[10]
$3s3p\ ^3P_2$	$3s3d\ ^3D_2$	235.05	234.78	5.20[09]	5.45[9]
$3s3p\ ^3P_2$	$3s3d\ ^3D_1$	235.62	235.32	5.68[08]	6.2 [8]
$3s3p\ ^1P_1$	$3s3d\ ^1D_2$	244.27	243.79	3.97[10]	4.19[10]
$3s^2\ ^1S_0$	$3s3p\ ^1P_1$	284.25	284.16	2.12[10]	2.2 [10]
$3s3p\ ^1P_1$	$3s3d\ ^3D_2$	305.35	304.99	2.20[07]	1.4 [7]
$3s3p\ ^1P_1$	$3s3d\ ^3D_1$	306.32	305.94	2.30[07]	2.4 [7]
$3s3p\ ^3P_1$	$3p^2\ ^3P_2$	292.32	292.27	4.38[09]	4.46[9]
$3s3p\ ^3P_0$	$3p^2\ ^3P_1$	302.37	302.33	6.72[09]	6.93[9]
$3s3p\ ^3P_2$	$3p^2\ ^3P_2$	304.95	304.89	1.24[10]	1.27[10]
$3s3p\ ^3P_1$	$3p^2\ ^3P_1$	307.80	307.73	4.76[09]	4.91[9]
$3s3p\ ^3P_1$	$3p^2\ ^3P_0$	317.65	317.60	1.72[10]	1.77[10]
$3s3p\ ^3P_2$	$3p^2\ ^3P_1$	321.84	321.77	6.90[09]	7.11[9]
$3s3p\ ^3P_1$	$3p^2\ ^1D_2$	312.03	312.56	1.03[09]	1.1 [9]
$3s3p\ ^3P_2$	$3p^2\ ^1D_2$	327.07	327.02	1.83[09]	2.0 [9]
$3s3p\ ^1P_1$	$3p^2\ ^1S_0$	325.05	324.97	1.94[10]	2.02[10]
$3s3d\ ^1D_2$	$3p3d\ ^1F_3$	333.67	332.85	1.68[10]	1.63[10]
$3s3s\ ^1S_0$	$3s3p\ ^3P_1$	417.22	417.26	3.70[07]	4.1 [7]
$3s3p\ ^1P_1$	$3p^2\ ^1D_2$	481.25	481.50	1.46[09]	1.55[9]
$3s3p\ ^1P_1$	$3p^2\ ^3P_2$	434.84	434.98	4.26[08]	4.7 [8]
$3s3p\ ^1P_1$	$3p^2\ ^3P_1$	470.01	470.17	7.51[06]	8.4 [6]
$3s3p\ ^1P_1$	$3p^2\ ^3P_0$	493.35	493.55	5.76[07]	6.4 [7]

one-electron QED contribution was made by fitting the QED contribution for Na-like ions given by Blundell [33]. The total QED correction for Mg-like ions is then given by the sum of the one-electron QED corrections, weighted by the eigenvectors obtained from MBPT calculations. Chen and Cheng [8] had a similar treatment of QED corrections using one-electron data obtained following the treatment described in Ref. [35].

In Table III, our MBPT results are also compared with MCDF calculations of the $3s^2\ ^1S_0$–$3s3p\ ^{1,3}P_J$ excitation energy recently presented by Jönsson and Froese Fisher in [3]. Our results are in precise agreement with the experimental NIST data [36] for $3s^2\ ^1S_0$–$3s3p\ ^3P_1$ transitions; the accuracy is about the same as found by Jönsson and Froese Fisher [3] for $Z=14$ and 15. For $3s^2\ ^1S_0$–$3s3p\ ^1P_1$ transitions, our data agree with data from [3] and [36] for $Z=13$, 16–18. The disagreement of our results with those from Ref. [3] for $Z=14$ and 15 is explained by the unsymmetric second-order energy contribution discussed in [34].

Energies of the $3pnl$ states are calculated for several high-Z Mg-like ions. We focus on three sets of results: measurements in iron by Shirai *et al.* [40] are compared with our results in Table V below. There is agreement to about 0.05–0.1 eV. Transition rates are also included in this table. Ekberg *et al.* [14] have made complete sets of measurements in ions with $Z=32$, 34, 38–40, which also show good agreement at the same level of accuracy. These tables are too lengthy to be included here, but are available at [15]. Finally, the wavelengths measured by Jupén *et al.* [17] in Kr ($Z=36$) and Mo ($Z=42$) are presented in Table VI below and found to be in good agreement with the present calculations.

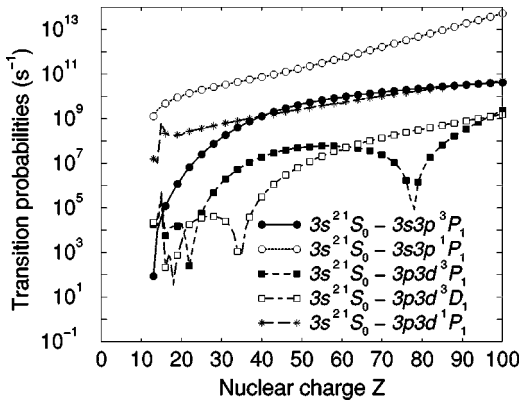

FIG. 5. Transition probabilities $A(3s^2\ ^1S_0$–$3l3l'\ ^{2S+1}L_1)$ as functions of Z.

B. Fine structure of the $3s3p$, $3s3d$, $3p3p$, and $3p3d$ triplets

The only measurements of fine-structure intervals were made by observing the wavelength differences between transitions within the triplet states. The intervals of both upper and lower states are overdetermined if all allowed transitions are observed, and this is the case for several ions in the sequence, particularly for the $3s3p$, $3s3d$, and $3p3p$ levels for lower Z. These fine structures are quite regular throughout the isoelectronic sequence, following the Landé interval rules reasonably well. Table IV shows that the splittings for $3s3p$ triplets, where measured, are in excellent agreement with our calculations.

On the other hand, our calculations show that the fine structures of the $3p3d$ levels do not follow the Landé rules for all Z. The P and D states are partially inverted, while the F states show regular ordering of the fine-structure splittings. In Fig. 4, we show how these two intervals vary strongly with nuclear charge for the P and D states. A few experimental data [36–41] are available to test our results. Some comparisons are made in Fig. 4. The unusual splittings are due principally to changes from LS to jj coupling, with mixing from other triplet and singlet states. States with different J states mix differently. Further experimental confirmation would be very helpful in verifying the correctness of these occasionally sensitive mixing parameters.

C. Transition rates and wavelengths in Mg-like ions

As mentioned previously, line strengths, oscillator strengths, and transition rates are calculated for all 168 allowed and forbidden electric dipole $3l_13l_2(LSJ)$-$3l_33l_4(L'S'J')$ transitions in Mg-like ions with nuclear

TABLE VI. Comparison of theoretical (a) and experimental (b) wavelength λ (Å) for Mg-like ions: Kr XXV and Mo XXXI: (a) present calculation, (b) Jupén *et al.* [17]. Numbers in brackets represent powers of 10.

		Kr XXV				Mo XXXI			
$l_1 l_2$ LSJ	$l_1' l_2' L'S'J'$	λ^a	λ^b	A^a (s^{-1})	Intensity[b]	λ^a	λ^b	A^a (s^{-1})	Intensity[b]
$3s3p\ ^1P_1$	$3p^2\ ^3P_0$	334.26		2.38[08]		325.70		1.76[08]	
$3s3p\ ^1P_1$	$3p^2\ ^1D_2$	274.11		2.61[09]		213.59		3.21[09]	
$3s3p\ ^1P_1$	$3p^2\ ^3P_1$	270.16		1.27[08]		211.02		3.65[08]	
$3s3p\ ^1P_1$	$3p^2\ ^3P_2$	216.93	217.03	2.13[09]	5	152.20		2.59[09]	
$3s3p\ ^3P_2$	$3p^2\ ^1D_2$	197.56		5.83[09]		158.20		8.47[09]	
$3s3p\ ^3P_2$	$3p^2\ ^3P_1$	195.50	195.63	1.29[10]	20	156.79		1.70[10]	
$3s3p\ ^3P_1$	$3p^2\ ^3P_0$	192.68		3.26[10]		155.25	155.34	4.32[10]	150
$3s3p\ ^1P_1$	$3p^2\ ^1S_0$	173.97		5.11[10]		124.43	124.54	9.31[10]	400
$3s3p\ ^3P_1$	$3p^2\ ^1D_2$	171.04	171.14	5.80[09]	70	124.18	124.32	1.30[10]	1300
$3s3p\ ^3P_1$	$3p^2\ ^3P_1$	169.49	169.61	1.17[10]	40	123.31	123.38	1.99[10]	350
$3s3p\ ^3P_2$	$3p^2\ ^3P_2$	166.02		2.81[10]		121.81	121.87	3.64[10]	1400
$3s3p\ ^3P_0$	$3p^2\ ^3P_1$	163.22	163.32	1.82[10]	60	117.86	117.90	3.31[10]	
$3s3p\ ^3P_1$	$3p^2\ ^3P_2$	146.88	146.92	1.15[10]	50	100.59	100.62	3.71[10]	3400
$3s3p\ ^3P_1$	$3p^2\ ^1S_0$	125.84		2.08[09]		87.66		3.55[09]	
$3s3p\ ^1P_1$	$3s3d\ ^3D_1$	183.42		3.05[08]		147.01		7.84[08]	
$3s3p\ ^1P_1$	$3s3d\ ^3D_2$	181.05		1.15[08]		143.29	143.10	2.01[07]	350
$3s3p\ ^3P_2$	$3s3d\ ^3D_1$	145.66		9.19[08]		118.46		1.13[09]	
$3s3p\ ^1P_1$	$3s3d\ ^1D_2$	145.63		7.80[10]		113.95		1.15[11]	
$3s3p\ ^3P_2$	$3s3d\ ^3D_2$	144.16		9.59[09]		116.03	115.92	2.31[10]	
$3s3p\ ^3P_2$	$3s3d\ ^3D_3$	141.79		3.68[10]		112.75		4.88[10]	
$3s3p\ ^3P_1$	$3s3d\ ^3D_1$	130.71		1.86[10]		98.30	98.24	2.78[10]	
$3s3p\ ^3P_1$	$3s3d\ ^3D_2$	129.50	129.42	3.52[10]	50	96.62		4.20[10]	800
$3s3p\ ^3P_0$	$3s3d\ ^3D_1$	126.95		2.87[10]		94.81		4.61[10]	
$3s3p\ ^3P_2$	$3s3d\ ^1D_2$	120.77		4.46[08]		96.01		3.30[09]	
$3s3p\ ^3P_1$	$3s3d\ ^1D_2$	110.31		3.82[09]		82.33		9.05[09]	
$3s3d\ ^3D_3$	$3p3d\ ^3F_4$	192.77		1.71[10]		135.95	136.18	3.35[10]	150
$3s3d\ ^1D_2$	$3p3d\ ^1F_3$	181.93		4.32[10]		133.23	133.26	7.55[10]	350

charges ranging from $Z=13$ to 100. Results were obtained in both length and velocity forms but only length-form results are tabulated since length-velocity differences are less than 1% for most cases.

Transition rates $A(s^{-1})$ for $3l_1 3l_2(LSJ)$-$3l_3 3l_4(L'S'J')$ lines are given in Figs. 5–7. Each figure shows transitions to a fixed LSJ state from states belonging to a *complex* of states $3l_3 3l_4(LS)$. A complex includes all states of the same parity and J obtained from combinations of $3l_3 3l_4(LS)$ states. For example, the odd-parity complex with $J=1$ includes states $3s3p\ ^3P_1$, $3s3p\ ^1P_1$, $3p3d\ ^3P_1$, $3p3d\ ^3D_1$, and $3p3d\ ^1P_1$

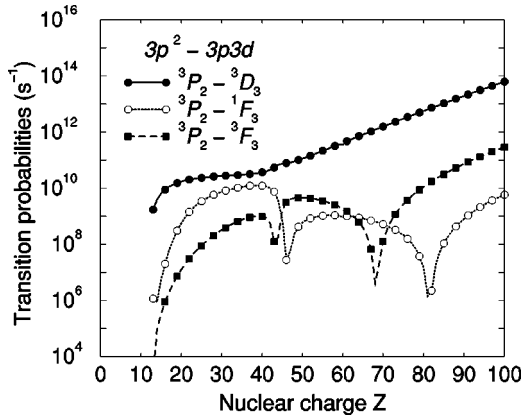

FIG. 6. Transition probabilities $A(3p^2\ ^3P_2-3p3d\ ^{2S+1}L_3)$ as functions of Z.

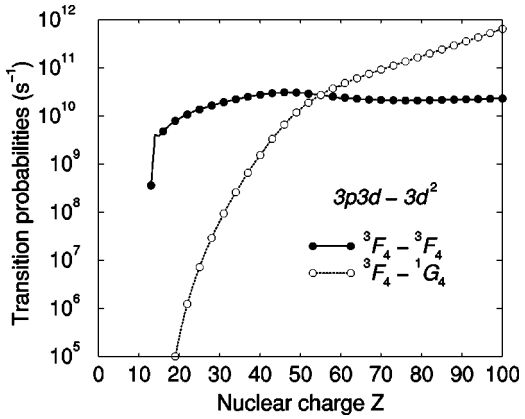

FIG. 7. Transition probabilities $A(3p3d\ ^3F_4-3d^2\ ^{2S+1}L_4)$ as functions of Z.

in LS coupling, or $3s3p_{1/2}(1)$,$3s3p_{3/2}(1)$,$3p_{1/2}3d_{3/2}(1)$, $3p_{3/2}3d_{3/2}(1)$, and $3p_{3/2}3d_{5/2}(1)$ in jj coupling. The LS designations are used below since they are more conventional. In Figs. 5 and 6, we present transition probabilities from levels of the odd-parity states with $J=1$ and $J=3$ into the even-parity states $3s^2\,{}^1S_0$ and $3p^2\,{}^3P_2$, respectively. Transition rates from the $3p3d\,{}^3F_4$ levels into the even-parity $J=4$ states are presented in Fig. 7.

It can be seen in Fig. 7 that the curves describing the $3p3d\,{}^3F_4$–$3d^2\,{}^3F_4$ and $3p3d\,{}^3F_4$–$3d^2\,{}^1G_4$ transitions are smooth provided that the label $3d^2\,{}^3F_4$ is changed into the label $3d^2\,{}^1G_4$ for $Z=54$ and 55. In Fig. 6, the singularity in the range of $Z=40$–50 is due to mixing of states inside the even-parity $J=2$ complex, as discussed in detail by Cheng and Johnson [1]. In Fig. 5, the singularity for small Z is explained by mixing of states inside the odd-parity $J=1$ complex. It is worth noting that the singularities occur when the A value for a given transition becomes very small compared to other A values within the same complex.

In Table V, wavelengths and electric dipole transition rates are presented for transitions in Mg-like Fe. We limit the table to those transitions given in [40]. The $3s3p$-$3s3d$ and $3s3p$-$3p^2$ transitions have been investigated, theoretically and experimentally, in greater detail than the $3p^2$-$3p3d$ transitions. The agreement between our MBPT wavelengths and the experimental values is within about 0.01–0.2 %. We also find good agreement between our transition rates and the experimental results of Ref. [40] for large A values (1%–5%) except for the $3p^2\,{}^1D_2$–$3p3d\,{}^1F_3$ transition. Even for the very small A values for the intercombination transitions, our values agree to within 10–20 % with NIST data [40].

The relative intensities observed by Jupén *et al.* [17] in Mg-like Kr and Mo also show reasonable agreement with our calculated A values (see Table VI). The ratios for intense spectral lines from [17] correspond well with our results for larger A values. Similarly, in the extensive work of Ekberg *et al.* [14] in Ge XXI, Se XXIII, Sr XXVII, Y XXVIII, and

TABLE VII. Lifetime (s) and oscillator strengths for the $3s3p\,{}^3P_1$ and ${}^1P_1$ levels for the Mg isoelectronic sequence: (a) present, (b) Curtis [7], (c) Huang and Johnson [4]. Numbers in brackets represent powers of 10.

	Lifetime				Oscillator strengths			
	$3s3p\,{}^3P_1$		$3s3p\,{}^1P_1$		$3s3p\,{}^3P_1$		$3s3p\,{}^1P_1$	
Z	a	b	a	b	a	c	a	c
14	1.01[−4]	5.99[−5]	4.29[−10]	4.10[−10]	1.60[−5]	2.44[−5]	1.59	1.70
15	2.65[−5]	1.81[−5]	2.95[−10]	2.75[−10]	3.64[−5]	5.26[−5]	1.31	1.57
16	8.40[−6]	6.72[−6]	2.13[−10]	2.02[−10]	7.73[−5]	9.84[−5]	1.30	1.45
17	3.75[−6]	2.88[−6]	1.66[−10]	1.57[−10]	1.24[−4]	1.68[−4]	1.22	1.35
18	1.71[−6]	1.37[−6]	1.35[−10]	1.27[−10]	2.03[−4]	2.68[−4]	1.14	1.26
19	8.55[−7]	7.05[−7]	1.13[−10]	1.06[−10]	3.14[−4]	4.07[−4]	1.07	1.18
20	4.83[−7]	3.85[−7]	1.01[−10]	8.99[−11]	4.37[−4]	5.94[−4]	0.960	1.11
21	2.57[−7]	2.24[−7]	8.33[−11]	7.75[−11]	6.83[−4]	8.40[−4]	0.970	1.05
22	1.54[−7]	1.35[−7]	7.30[−11]	6.77[−11]	9.47[−4]	1.15[−3]	0.918	0.992
23	9.52[−8]	8.45[−8]	6.49[−11]	5.98[−11]	1.28[−3]	1.55[−3]	0.875	0.944
24	6.13[−8]	5.47[−8]	5.78[−11]	5.32[−11]	1.70[−3]	2.04[−3]	0.837	0.901
25	4.05[−8]	3.64[−8]	5.21[−11]	4.76[−11]	2.22[−3]	2.63[−3]	0.802	0.862
26	2.75[−8]	2.50[−8]	4.72[−11]	4.29[−11]	2.84[−3]	3.33[−3]	0.771	0.827
27	1.92[−8]	1.74[−8]	4.27[−11]	3.88[−11]	3.57[−3]	4.17[−3]	0.743	0.795
28	1.36[−8]	1.25[−8]	3.89[−11]	3.52[−11]	4.43[−3]	5.13[−3]	0.718	0.767
29	9.90[−9]	9.08[−9]	3.55[−11]	3.21[−11]	5.43[−3]	6.24[−3]	0.694	0.741
30	7.30[−9]	6.72[−9]	3.25[−11]	2.93[−11]	6.55[−3]	7.49[−3]	0.673	0.717
31	5.46[−9]	5.07[−9]	2.97[−11]	2.68[−11]	7.82[−3]		0.654	
32	4.17[−9]	3.88[−9]	2.72[−11]	2.45[−11]	9.23[−3]		0.636	
33	3.23[−9]	3.03[−9]	2.50[−11]	2.25[−11]	1.08[−2]		0.620	
34	2.54[−9]	2.39[−9]	2.29[−11]	2.06[−11]	1.24[−2]		0.605	
35	2.02[−9]	1.91[−9]	2.11[−11]	1.89[−11]	1.42[−2]	1.58[−2]	0.591	0.624
36	1.63[−9]	1.54[−9]	1.94[−11]	1.74[−11]	1.61[−2]	1.78[−2]	0.578	0.609
37	1.34[−9]	1.26[−9]	1.78[−11]	1.60[−11]	1.80[−2]		0.566	
38	1.11[−9]	1.05[−9]	1.64[−11]	1.47[−11]	2.00[−2]		0.556	
39	9.26[−10]	8.78[−10]	1.50[−11]	1.35[−11]	2.21[−2]		0.546	
40	7.81[−10]	7.43[−10]	1.38[−11]	1.23[−11]	2.42[−2]		0.537	
41	6.67[−10]	6.37[−10]	1.26[−11]	1.13[−11]	2.62[−2]		0.529	
42	5.75[−10]	5.49[−10]	1.16[−11]	1.03[−11]	2.83[−2]		0.521	

TABLE VIII. Theoretical lifetime data (ns) for all singlet states in the $n=3$ complex of the Mg sequence for $Z\leqslant 26$: (a) present calculation, (b) Froese Fisher and Godefroid [2].

Z		$3p^2\,{}^1S_0$	$3d^2\,{}^1S_0$	$3s3p\,{}^1P_1$	$3p3d\,{}^1P_1$	$3p^2\,{}^1D_2$	$3s3d\,{}^1D_2$	$3d^2\,{}^1D_2$	$3p3d\,{}^1D_2$	$3p3d\,{}^1F_3$	$3d^2\,{}^1G_4$
13	a	0.840	0.775	0.800	0.898	6900	0.813	0.206	0.808	0.0030	79.9
13	b	0.97		0.70		2381	0.75		0.81		
14	a	0.476	0.232	0.429	0.443	45.7	0.232	0.150	0.380	0.305	104
14	b	0.40		0.39	0.51	39.5	0.22		0.41	0.42	
15	a	0.325	0.136	0.295	0.162	27.9	0.143	0.164	0.272	0.163	12.9
15	b	0.32		0.26	0.16	11.9	0.12	0.29	0.27	0.16	1.2
16	a	0.243	0.0581	0.213	0.122	6.53	0.0980	0.0785	0.201	0.103	0.599
16	b	0.24	0.098	0.20	0.12	5.9	0.085	0.11	0.20	0.087	0.35
17	a	0.191	0.0549	0.166	0.0907	3.32	0.0741	0.0634	0.159	0.0772	0.271
17	b	0.19	0.18	0.15	0.073	3.6	0.087	0.060	0.15	0.064	0.26
18	a	0.156	0.0459	0.135	0.0725	2.30	0.0625	0.0523	0.131	0.0629	0.174
18	b	0.15	0.044	0.13	0.061	2.5	0.056	0.053	0.13	0.053	0.17
19	a	0.131	0.0385	0.114	0.0604	1.52	0.0523	0.0437	0.112	0.0527	0.128
19	b	0.13	0.037	0.11	0.053	1.9	0.048	0.046	0.11	0.043	0.13
20	a	0.112	0.0073	0.101	0.0524	1.06	0.0454	0.0375	0.0978	0.0455	0.102
20	b	0.11	0.033	0.093	0.047	1.5	0.042	0.039	0.095	0.040	0.10
21	a	0.0980	0.0253	0.0833	0.0449	0.766	0.0401	0.0329	0.0870	0.0401	0.0846
22	a	0.0869	0.0244	0.0730	0.0399	0.571	0.0359	0.0292	0.0782	0.0359	0.0723
22	b	0.086	0.025	0.073	0.038	1.0	0.035	0.032	0.076	0.032	0.073
23	a	0.0774	0.0224	0.0649	0.0358	0.439	0.0325	0.0261	0.0712	0.0324	0.0631
24	a	0.0698	0.0204	0.0581	0.0325	0.348	0.0296	0.0237	0.0650	0.0296	0.0559
24	b	0.070	0.021	0.060	0.032	0.75	0.030	0.027	0.064	0.028	0.057
25	a	0.0635	0.0188	0.0521	0.0296	0.283	0.0271	0.0218	0.0596	0.0271	0.0501
26	a	0.0583	0.0173	0.0472	0.0272	0.235	0.0250	0.0202	0.0550	0.0250	0.0454
26	b	0.059	0.018	0.051	0.028	0.60	0.026	0.023	0.055	0.024	0.048

Zr XXIX, the ratios for intense lines correspond well with our theoretical A values; however, for other transitions with large A values there are no experimental measurements.

D. Lifetimes in Mg-like ions

A limited subset of our lifetime calculations is presented below to compare with available theoretical and experimental data. Lifetimes for the $3s^2$-$3s3p$ resonance and intercombination transitions were reported by Curtis [7]: he used measured lifetimes and spectroscopic energy levels as input to obtain semiempirical values for lifetimes along the Mg isoelectronic sequence. In Table VII, the semiempirical lifetimes for these two levels are compared with results from our present calculation. Our data are found to be systematically larger those from [7] for the entire interval $Z=14$–42. Our results for oscillator strengths are also compared with the MCRRPA calculations of Ref. [4] in this table. Our oscillator strengths are seen to be systematically smaller than those from [4]; however, our values come into agreement with

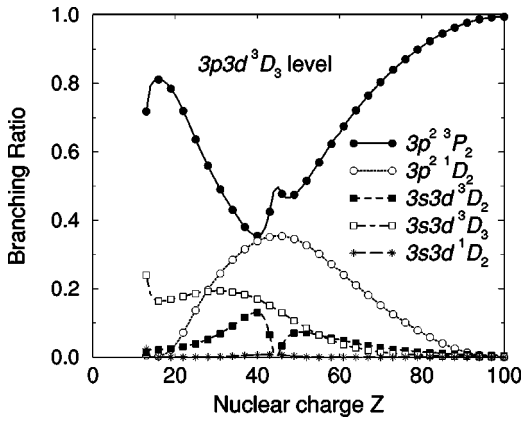

FIG. 8. Channel contributions to the $3p3d\,{}^3D_3$ lifetime as functions of Z.

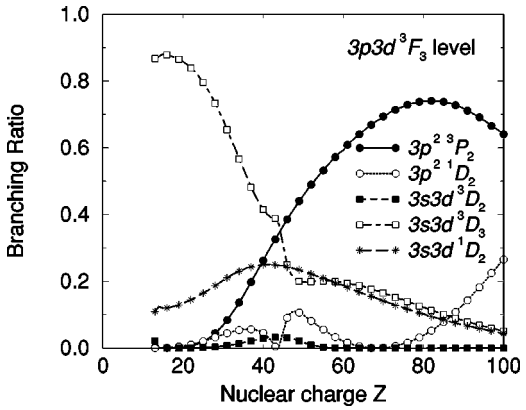

FIG. 9. Channel contribution in the $3p3d\,{}^3F_3$ lifetime as functions of Z.

TABLE IX. Theoretical lifetime data (ns) for the triplet states in the $n=3$ complex for Mg-like ions, $Z=13$–26.

Z	$3p3d\,^3P_0$	$3p3d\,^3P_1$	$3p3d\,^3P_2$	$3p3d\,^3D_1$	$3p3d\,^3D_2$	$3p3d\,^3D_3$	$3p3d\,^3F_2$	$3p3d\,^3F_3$	$3p3d\,^3F_4$	$3d^2\,^3F_4$
13	0.838	0.629	0.636	0.435	0.437	0.424	0.0362	0.0386	0.0442	0.306
14	0.312	0.313	0.315	0.207	0.208	0.208	22.5	24.9	25.7	0.168
15	0.195	0.195	0.196	0.129	0.129	0.129	2.80	2.85	2.82	0.178
16	0.139	0.139	0.140	0.0926	0.0930	0.0926	1.46	1.49	1.47	0.115
17	0.108	0.106	0.108	0.0735	0.0736	0.0728	0.972	1.00	0.980	0.0860
18	0.0881	0.0839	0.0872	0.0620	0.0615	0.0601	0.709	0.744	0.725	0.0690
19	0.0741	0.0672	0.0722	0.0550	0.0533	0.0516	0.544	0.584	0.568	0.0579
20	0.0639	0.0548	0.0611	0.0506	0.0474	0.0451	0.431	0.476	0.459	0.0500
21	0.0557	0.0459	0.0528	0.0467	0.0430	0.0400	0.352	0.399	0.382	0.0441
22	0.0495	0.0400	0.0462	0.0431	0.0392	0.0360	0.293	0.338	0.323	0.0395
23	0.0443	0.0354	0.0411	0.0395	0.0360	0.0328	0.248	0.292	0.276	0.0358
24	0.0397	0.0318	0.0371	0.0362	0.0332	0.0299	0.215	0.255	0.239	0.0328
25	0.0360	0.0290	0.0336	0.0332	0.0307	0.0276	0.188	0.224	0.209	0.0302
26	0.0328	0.0265	0.0309	0.0305	0.0284	0.0255	0.167	0.197	0.184	0.0279

Z	$3p^2\ ^3P_0$	$3p^2\,^3P_1$	$3p^2\,^3P_2$	$3s3d\,^3D_1$	$3s3d\,^3D_2$	$3s3d\,^3D_3$	$3d^2\,^3P_0$	$3d^2\,^3P_1$	$3d^2\,^3P_2$	$3d^2\,^3F_2$	$3d^2\,^3F_3$
13	1.42	0.831	0.694	0.862	0.864	0.870	0.559	0.591	0.405	0.202	0.307
14	0.465	0.474	0.421	0.374	0.374	0.377	0.189	0.210	0.108	0.142	0.165
15	0.344	0.324	0.295	0.226	0.228	0.229	0.123	0.141	0.0748	0.153	0.177
16	0.218	0.242	0.223	0.162	0.163	0.164	0.0702	0.0805	0.0600	0.0915	0.114
17	0.177	0.189	0.177	0.126	0.128	0.129	0.0603	0.0699	0.0541	0.0668	0.0851
18	0.143	0.154	0.146	0.104	0.105	0.107	0.0500	0.0582	0.0403	0.0527	0.0681
19	0.117	0.129	0.124	0.0887	0.0898	0.0917	0.0426	0.0496	0.0365	0.0437	0.0570
20	0.0636	0.110	0.107	0.0774	0.0787	0.0806	0.0362	0.0434	0.0324	0.0373	0.0491
21	0.0997	0.0960	0.0941	0.0687	0.0702	0.0719	0.0329	0.0382	0.0291	0.0325	0.0431
22	0.0836	0.0845	0.0838	0.0617	0.0628	0.0654	0.0295	0.0344	0.0265	0.0288	0.0385
23	0.0725	0.0749	0.0755	0.0559	0.0572	0.0595	0.0267	0.0311	0.0244	0.0258	0.0348
24	0.0644	0.0671	0.0684	0.0510	0.0526	0.0549	0.0243	0.0283	0.0225	0.0233	0.0317
25	0.0571	0.0604	0.0622	0.0468	0.0484	0.0510	0.0223	0.0258	0.0208	0.0213	0.0290
26	0.0511	0.0547	0.0569	0.0431	0.0446	0.0474	0.0206	0.0239	0.0192	0.0195	0.0267

TABLE X. Comparison of theoretical and experimental lifetimes (ns) for Mg-like ions.

	$Z=17$		$Z=18$		$Z=20$	
Level	τ_{theor}	τ_{exp} [18]	τ_{theor}	τ_{exp} [44]	τ_{theor}	τ_{exp} [25]
$3s3p(^1P)$	0.166	0.165±0.009	0.135	0.144±0.015	0.101	0.100±0.010
$3p^2(^1D)$	3.32	2.85±0.1	2.30	1.72±0.15	1.06	0.840±0.060
$3p^2(^1S)$	0.191	0.24±0.03	0.156		0.112	0.150±0.008
$3s3d(^1D)$	0.0741	0.064±0.004	0.0625	0.083±0.010	0.0454	0.072±0.003
$3p3d(^1D)$	0.159	0.19±0.03	0.131		0.0978	
$3p3d(^1F)$	0.077	0.080±0.01	0.0629		0.0455	
$3p^2(^3P_2)$	0.177		0.146	0.152±0.010	0.107	0.134±0.008
$3p^2(^3P_1)$	0.189		0.154	0.159±0.010	0.110	
$3s3d(^3D_2)$	0.128		0.105	0.110±0.010	0.0787	0.100±0.015
$3s3d(^3D_3)$	0.129		0.107	0.112±0.010	0.0806	0.117±0.009
$3p3d(^3D_3)$	0.0728		0.0601	0.083±0.010	0.451	
$3p3d(^3F_2)$	0.972		0.709		0.431	0.653±0.063
$3p3d(^3F_3)$	1.00		0.749		0.476	0.473±0.021
$3p3d(^3F_4)$	0.980		0.725		0.459	0.513±0.040

those from Ref. [4] if we restrict our model space to include only s and p orbitals.

Froese Fisher and Godefroid [2] presented theoretical lifetime data for all singlet states in the $n=3$ complex for $Z \leqslant 26$. Their calculations include only LS-allowed transitions; the calculations of [2] are compared with our MBPT data in Table VIII and agreement is found at the 10% level except for the level $3p^2\,{}^1D_2$. Earlier, Cheng and Johnson [1] discussed very large mixing in the even-parity complex with $J=2$, showing that there is only a small energy difference between the $3p^2\,{}^1D_2$ and $3p^2\,{}^3P_2$ levels, and these two levels should be treated together. Such a treatment is not possible in a pure LS-coupling scheme. The disagreement for the $3p^2\,{}^1D_2$ level increases with increasing Z, confirming our conclusion about the cause of the difference.

In Table IX, a limited set of our MPBT data is presented for triplet states of Mg-like ions up to $Z=26$. The difference in the lifetimes of the individual multiplet levels is about 10%. This is especially true for the low-lying states $3p^2$ and $3s3d$. However, differences in lifetimes of individual multiplet levels for $3d^2$ states are about 50%.

The contributions of different channels to the lifetimes of the $3p3d\,{}^3D_3$ and $3p3d\,{}^3F_3$ levels are shown in Figs. 8 and 9. The curves represent the ratios of individual transition probabilities A to the sum of all transition probabilities ΣA for the level considered. It is seen from Fig. 8 that the largest contribution to the lifetime of the $3p3d\,{}^3D_3$ level is from the $A(3p^2\,{}^3P_2-3p3d\,{}^3D_3)$ channel. The $A(3s3d\,{}^3D_3-3p3d\,{}^3D_3)$ gives about 25%–10% of the lifetime value for Z up to 40. The $A(3p^2\,{}^1D_2-3p3d\,{}^3D_3)$ channel contributes about 20%–35% in the range $Z=30$–60.

There are two main channels for the lifetime of the $3p3d\,{}^3F_3$ level: $A(3s3d\,{}^3D_3-3p3d\,{}^3F_3)$ and $A(3p^2\,{}^3P_2-3p3d\,{}^3F_3)$. It is also seen in Fig. 9 that the two curves $A(3s3d\,{}^3D_3-3p3d\,{}^3F_3)/\Sigma A$ and $A(3p^2\,{}^3P_2-3p3d\,{}^3F_3)/\Sigma A$ cross between $Z=42$ and $Z=43$. An additional contribution to the lifetime of the $3p3d\,{}^3F_3$ level of about 10%–20% comes from the intercombination channel $A(3s3d\,{}^1D_2-3p3d\,{}^3F_3)$ for all Z.

There also exist a few lifetime measurements for highly charged ions of the Mg sequence.

a. Pb: Weak Ne-like and Mg-like lines of lead were observed near 800 eV in an accelerator-based experiment by Simonovici *etal.* [42]. They identified a peak at 791.90 ± 0.29 eV as the $3s3d_{3/2}(2)$-$3p_{3/2}3d_{3/2}(3)$ transition. Our calculations give 791.50 eV. However, our calculations also predict the transition $E[3s3d_{3/2}(2)$-$3p_{3/2}3d_{3/2}(1)]$ at 792.09 eV.

b. Xe and Au: In beam-foil measurements in Xe and Au [43], the $3s^2\,{}^1S_0$-$3s3p\,{}^{1,3}P_1$ transitions were observed and lifetimes measured. Experimental results for Xe ($\lambda_{\rm exp}=6.2895$ nm, $\tau_{\rm exp}=5\pm1.5$ ps and $\lambda_{\rm exp}=12.992$ nm, $\tau_{\rm exp}=170\pm30$ ps) are in good agreement with our calculated values ($\lambda_{\rm theor}=6.286$ nm, $\tau_{\rm theor}=3.64$ ps and $\lambda_{\rm theor}=12.980$ nm, $\tau_{\rm theor}=163$ ps) but disagree for Au ($\lambda_{\rm exp}=6.805$ nm, $\tau_{\rm exp}=25\pm5$ ps, $\lambda_{\rm theor}=7.1806$ nm, and $\tau_{\rm theor}=45.6$ ps).

c. Br: A beam-foil lifetime measurement for the intercombination transition in Br^{23+} has been reported [24]. The difference between experiment and theory is about 10% ($\tau_{\rm exp}=1.86\pm0.15$ ns and $\tau_{\rm theor}=2.02$ ns).

Several lower-Z lifetime measurements have also been reported in chlorine [18], in argon [44], and in calcium [25].

In Table X, MBPT lifetime values are compared with the available experimental data. Good agreement with experimental data for the $3s3p\,{}^1P_1$ level is found. For other levels, the disagreement between theoretical and experimental data is about 20%. For many levels, except the $3p^2\,{}^1D_2$ level, the theoretical lifetimes are smaller than experimental values.

IV. CONCLUSION

In summary, a systematic second-order MBPT study of the energies of the $n=3$ states of Mg-like ions has been presented. These calculations are found to differ from existing experimental energy data for intermediate Z at the level of 50 $\rm cm^{-1}$ for triplet states and 500 $\rm cm^{-1}$ for singlet states. They provide a smooth theoretical reference database for line identification.

Also presented is a systematic second-order relativistic MBPT study of reduced matrix elements, oscillator strengths, and transition rates for allowed and forbidden $3l$-$3l'$ electric-dipole transitions in Mg-like ions with nuclear charges ranging from $Z=13$ to 100. The retarded dipole matrix elements include correlation corrections from Coulomb and Breit interactions. Contributions from negative-energy states were also included in the second-order matrix elements. Both length and velocity forms of the matrix elements were evaluated, and small differences, caused by the nonlocality of the starting Hartree-Fock potential, were found between the two forms. Second-order MBPT transition energies were used to evaluate oscillator strengths and transition rates.

Our theoretical data for allowed transitions agree with experiment within the experimental uncertainties for the $3s3p\,{}^1P_1$ level. We believe that our results will be useful in analyzing existing experimental data and planning new experiments. There remains a paucity of experimental data for many of the higher ionized members of this sequence, both for term energies and for transition probabilities and lifetimes. Additionally, the matrix elements from the present calculations will provide basic theoretical input for calculations of reduced matrix elements, oscillator strengths, and transition rates in three-electron Al-like ions.

ACKNOWLEDGMENTS

The work of W.R.J. was supported in part by National Science Foundation Grant No. PHY-99-70666. U.I.S. acknowledges partial support by Grant No. B503968 from Lawrence Livermore National Laboratory.

[1] K.T. Cheng and W.R. Johnson, Phys. Rev. A **16**, 263 (1977).
[2] C. Froese Fisher and M. Godefroid, Nucl. Instrum. Methods Phys. Res. **202**, 307 (1982).
[3] P. Jönsson and C. Froese Fisher, J. Phys. B **30**, 5861 (1997).
[4] K.-N. Huang and W.R. Johnson, Nucl. Instrum. Methods Phys. Res. B **9**, 502 (1985).
[5] H.-S. Chou, H.-C. Chi, and K.-N. Huang, J. Phys. B **26**, 4079 (1993).
[6] K. Butler, C. Mendoza, and C.J. Zeippen, J. Phys. B **26**, 4409 (1993).
[7] L.J. Curtis, Phys. Scr. **43**, 137 (1991).
[8] M.H. Chen and K.T. Cheng, Phys. Rev. A **55**, 3440 (1997).
[9] B.C. Fawcett, At. Data Nucl. Data Tables **28**, 557 (1983).
[10] U. Litzén and A. Redfors, Phys. Lett. A **127**, 88 (1988).
[11] S.S. Churilov, V.E. Levashov, and J.F. Wyart, Phys. Scr. **40**, 625 (1989).
[12] J. Sugar and V. Kaufman, J. Opt. Soc. Am. B **3**, 704 (1986).
[13] J. Sugar and V. Kaufman, Phys. Scr. **34**, 797 (1986).
[14] J.O. Ekberg, U. Feldman, J.F. Seely, and C.M. Brown, Phys. Scr. **40**, 643 (1989).
[15] See EPAPS Document No. E-PLRAAN-61-044005 for comparisons of theoretical wavelengths in the Mg-like ions Ge XXI, Se XXIII, Sr XXVII, Y XXVIII, and Zr XXIX with experimental data from Ekberg *et al.* [14]. This document may be retrieved via the EPAPS homepage (http://www.aip.org/pubservs/epaps.html) or from ftp.aip.org in the directory /epaps/. See the EPAPS homepage for more information.
[16] J.F. Seely, J.O. Ekberg, U. Feldman, J. Schwob, S. Suckewer, and A. Wouters, J. Opt. Soc. Am. B **B5**, 602 (1988).
[17] C. Jupén, B. Denne, and I. Martinson, Phys. Scr. **41**, 669 (1990).
[18] L. Engström, P. Bengtsson, C. Jupén, A.E. Livingston, and I. Martinson, Phys. Rev. A **51**, 179 (1995).
[19] N. Reistad, C. Jupén, S. Huldt, L. Engström, and I. Martinson, Phys. Scr. **32**, 164 (1985).
[20] N. Reistad, L. Engström, and H.G. Berry, Phys. Scr. **34**, 158 (1986).
[21] R. Hutton, L. Engström, and E. Träbert, Nucl. Instrum. Methods Phys. Res. B **31**, 294 (1988).
[22] R. Hutton, N. Reistad, I. Martinson, E. Träbert, P.H. Heckmann, J.H. Blanke, H.M. Hellmann, and R. Hucke, Phys. Scr. **35**, 300 (1987).
[23] Y. Baudinet-Robinet, P.D. Dumont, and H.P. Garnir, Nucl. Instrum. Methods Phys. Res. **202**, 33 (1982).
[24] E. Träbert, J. Suleiman, S. Cheng, H.G. Berry, R.W. Dunford, E.P. Kanter, C. Kurtz, A.E. Livingston, K.W. Kukla, F.G. Serpa, and L.J. Curtis, Phys. Rev. A **47**, 3805 (1993).
[25] E. Träbert, E.H. Pinnington, J.A. Kernahan, J. Doerfert, J. Granzow, P.H. Heckmann, and R. Hutton, J. Phys. B **29**, 2647 (1996).
[26] M.S. Safronova, W.R. Johnson, and U.I. Safronova, Phys. Rev. A **53**, 4036 (1996).
[27] U.I. Safronova, W.R. Johnson, M.S. Safronova, and A. Derevianko, Phys. Scr. **59**, 286 (1999).
[28] U.I. Safronova, A. Derevianko, M.S. Safronova, and W.R. Johnson, J. Phys. B **32**, 3527 (1999).
[29] G.E. Brown and D.E. Ravenhall, Proc. R. Soc. London, Ser. A **208**, 552 (1951).
[30] J. Sucher, Phys. Rev. A **22**, 348 (1980), and references therein.
[31] M.H. Mittleman, Phys. Rev. A **4**, 893 (1971); **5**, 2395 (1972); **24**, 1167 (1981).
[32] A. Derevianko, I.M. Savukov, W.R. Johnson, and D.R. Plante, Phys. Rev. A **58**, 4453 (1998).
[33] S.A. Blundell, Phys. Rev. A **47**, 1790 (1993).
[34] M.S. Safronova, W.R. Johnson, and U.I. Safronova, J. Phys. B **30**, 2375 (1997).
[35] K.T. Cheng, W.R. Johnson, and J. Sapirstein, Phys. Rev. A **47**, 1817 (1993); Phys. Rev. Lett. **66**, 2960 (1991).
[36] C. E. Moore, *Atomic Energy Levels*, Natl. Bur. Stand. Ref. Data Ser., Natl. Bur. Stand (U.S.) Circ. No. 35 (U.S. GPO, Washington, D.C., 1971).
[37] T. Shirai, T. Nakagaki, J. Sugar, and W.L. Wiese, J. Phys. Chem. Ref. Data **21**, 273 (1992).
[38] T. Shirai, Y. Nakai, T. Nakagaki, J. Sugar, and W.L. Wiese, J. Phys. Chem. Ref. Data **22**, 1279 (1993).
[39] T. Shirai, T. Nakagaki, K. Okazaki, J. Sugar, and W.L. Wiese, J. Phys. Chem. Ref. Data **23**, 179 (1994).
[40] T. Shirai, Y. Funatake, K. Mori, J. Sugar, W.L. Wiese, and Y. Nakai, J. Phys. Chem. Ref. Data **19**, 127 (1990).
[41] T. Shirai, A. Mengoni, Y. Nakai, K. Mori, J. Sugar, W.L. Wiese, K. Mori, and N. Sakai, J. Phys. Chem. Ref. Data **21**, 23 (1992).
[42] A. Simionovici, D.D. Dietrich, R. Keville, T. Cowan, P. Beiersdorfer, M.H. Chen, and S.A. Blundell, Phys. Rev. A **48**, 3056 (1993).
[43] E. Träbert, J. Doerfert, J. Granzow, R. Büttner, U. Staude, K.-H. Schartner, P. Rymuza, L. Engström, and R. Hutton, Z. Phys. D: At., Mol. Clusters **32**, 295 (1995).
[44] M.-C. Buchet-Poulizac, J.-P. Buchet, and P. Ceyzeriat, Nucl. Instrum. Methods Phys. Res. **202**, 13 (1982).